Sustainable Energy Technologies and Assessments 57 (2023) 103250

Contents lists available at ScienceDirect

Sustainable Energy Technologies and Assessments

journal homepage: www.elsevier.com/locate/seta

Aerodynamic performance optimization of vertical axis wind turbine with straight blades based on synergic control of pitch and flap

Zhaolong Han [a,b], Hao Chen [a], Yaoran Chen [a], Jie Su [a], Dai Zhou [a,*], Hongbo Zhu [a], Tangbin Xia [c], Jiahuang Tu [d]

[a] State Key Laboratory of Ocean Engineering, School of Naval Architecture, Ocean and Civil Engineering, Shanghai Jiao Tong University, Shanghai 200240, People's Republic of China
[b] Institute of Polar and Ocean Technology, Institute of Marine Equipment, Shanghai Jiao Tong University, Shanghai 200240, People's Republic of China
[c] State Key Laboratory of Mechanical System and Vibration, School of Mechanical Engineering, Shanghai Jiao Tong University, SJTU-Fraunhofer Center, Shanghai 200240, People's Republic of China
[d] College of Civil Engineering and Mechanics, Xiangtan University, Xiangtan 411105, Hunan Province, People's Republic of China

A R T I C L E I N F O

Keywords:
Vertical axis wind turbine
Variable pitch and flap
Orthogonal experimental design
Flow structure
Aerodynamic performance

A B S T R A C T

Low power efficiency is a critical reason that restricts the potential application of the vertical axis wind turbine (VAWT) in offshore engineering. Hence, efficiency enhancement is an essential topic for the VAWT design. This paper attempts to propose an improved active control strategy and a novel blade structure with a trailing-edge flap for H-type VAWT to improve the power outputs at different tip speed ratios (TSRs). The orthogonal experiment design (OED) method was applied to optimize the motion of pitch and flap at low and moderate TSRs. Subsequently, the output characteristics, including the coefficients of power, torque, tangential force, and thrust of the optimized pitch-flap (P-F) model and three other models, namely the base model, the pitch-only (P-O) model, and the flap-only (F-O) model, were compared. Besides, the flow structures and static pressure distribution on the blade surface were studied to reveal the mechanism of power increase. It was found that the synergic motion of pitch and flap could effectively suppress the flow separation and delay the dynamic stall around blade. The result indicated that enhancement of the P-F model in torque coefficient was over 130% and 60% at low and moderate TSRs compared to the base model. In addition, the synergic motion of pitch and flap was found able to reduce the load fluctuation of the VAWT. The improved active control strategy and the blade structure with a trailing-edge flap may be helpful for the potential application of the H-type VAWT in offshore engineering.

Introduction

Ocean wind energy is one of the most promising sustainable alternative sources for expansion in the foreseeable future because of the abundant energy resources, clean production, and easy availability [1,2]. The wind turbine is the most critical component of a wind energy system, whose configuration directly affects the efficiency of converting wind energy into electricity. Modern wind turbine system mainly consists of two categories, namely horizontal axis wind turbine (HAWT) and vertical axis wind turbine (VAWT) according to the axial rotational direction [3]. The HAWT remains the most widely used type due to its higher power generation efficiency and reliable technology. Currently, the commercial power of the offshore HAWT can be up to 8 MW [4]. For VAWT, with further exploitation of offshore wind resources, it is receiving renewed concern, especially in the offshore environment, because of the advantages of structural simplicity, offshore floating suitability, and scalability [5–7].

At present, the low conversion efficiency of VAWT is the key factor to restrict the large-scale development of vertical axis wind turbines. The periodic change of blade attack angle will lead to dynamic stall and complex unsteady flows around blades. In this aspect, great effort has been made to overcome the aerodynamic disadvantages of conventional VAWT. The effects of rotor solidity [8,9], blade configuration [10,11], and pitch angle [12] on aerodynamic characteristics of the VAWTs were investigated to determine the best settings for VAWT. In addition, leading-edge micro-cylinder [13,14], slotted airfoil [15,16], vortex generators [17], and other passive flow-control technology are widely

* Corresponding author.
E-mail address: zhoudai@sjtu.edu.cn (D. Zhou).

https://doi.org/10.1016/j.seta.2023.103250
Received 21 April 2022; Received in revised form 7 March 2023; Accepted 24 April 2023

Nomenclature

Abbreviation and Symbols

HAWT	Horizontal Axis Wind Turbine
VAWT	Vertical Axis Wind Turbine
DMST	Double Multiple Stream Tube
TSR	Tip Speed Ratio
OED	Orthogonal Experiment Design
P-F	Pitch-flap
P-O	Pitch-only
F-O	Flap-only
FDG	Flow Deflecting Gap
CFD	Computational Fluid Dynamics
AOA	Angle of Attack
SIMPLE	Semi-Implicit Method for Pressure Linked Equations
D	Diameter
C	Chord length
σ	Solidity
A	Swept area
W	Relative local velocity
Θ	Azimuthal angle of the blade
λ	Tip speed ratio
U_∞	Freestream velocity
ω	Angular velocity
F_T	Tangential force
F_N	Normal force
C_T	Tangential force coefficient
C_N	Normal force coefficient
ρ	Air density
H	Span length
C_Q	Torque coefficient
C_P	Power coefficient
Q	Torque
R	Radius
C_{thrust}	Thrust coefficient
F_{thrust}	Thrust
β_p	Pitch angle
β_f	Flap deflection angle
x_p	Distance from the leading-edge to the rotate center
x_f	Distance from the leading-edge to the rotational center of the flap
α	Angle of Attack
α'	Equivalent angle of attack
ξ	Ratio of power coefficient C_P and thrust coefficient C_{thrust}
Re	Reynolds number

used to improve the stall characteristic of VAWT. However, the optimizing strategies should be different under different flow field conditions. The limitation of these optimization and flow-control strategies is that these strategies are hard to accommodate with different ambient flow conditions.

Recently, the active control strategies represented by variable blade pitch are widely used in VAWT. It was found that the controlling the pich angle of wind turbine blade can improve the aerodynamic performance of VAWTs, as well as the load distribution on the blades [18]. Several studies have focused on forcing the blades to do specified pitch motion while rotating. Sagharichi et al. [19] selected four pitch functions with four amplitudes: 0°, 3°, 10°, and 20° to analyze the relationship between the angle of attack and self-starting performance of an H-type VAWT. The results show that the amplitude of 3° has better performance than other amplitudes. Chen et al. [20] compared the performance of a fixed-blade vertical axis turbine with a variable pitch turbine, whose blades were forced to do sinusoidal pitching motions during rotation. The results showed that not only the power efficiency of the turbine increase, but also the fluctuations in power output, rotation speed, and torque outputs were suppressed. Jain and Abhishek [21] developed an aerodynamic model based on the Double Multiple Stream Tube (DMST) for a small-scale VAWT. The study found that the suitable amplitude of sinusoidal blade pitch was around 10° when TSRs were higher than 2.0 and increased to 35° when the TSRs were less than 0.5. There were also some new optimization methods for pitch control with the help of machine learning techniques [22,23].

However, for large-scale VAWT, the pitch control of a large blade generally demands more power and needs to spend relatively longer times to start and brake. Aimed at this problem, an effective solution is proposed by using flaps. Early flaps were widely used in aviation-related fields to increase the lift-to-drag ratio and delay stall at high angles of attack [24,25]. In recent years, flap control as an effective method to reduce blade load and increase blade lift has got a great evolution in the application of VAWT. Zhu et al. [26] designed three kinds of novel flow deflecting gap (FDG) blades. The results showed that compared with the clean blade, the FDG blade increased the lift-to-drag ratio of blades at a high angle of attack. Hao et al. [27] investigated the adaptive flap in terms of improving its performance on VAWT. The results showed that when TSR = 0.6 and 1.2, the flap significantly improved the power coefficient and relieved the flow separation in VAWT. Liu et al. [28] investigated the effects of the trailing-edge flap on the aerodynamic performance of NACA0018 airfoil and VAWT. The results showed that when TSR = 1.3 and TSR = 1.4, the power coefficients of VAWT blades with trailing-edge flaps increased by 24.2% and 23.7% compared with VAWT without trailing-edge flap.

While the concept of individual pitch control and trailing edge flaps have been put forward in HAWT to reduce flapwise fatigue loads on wind turbine blades [29], the relevant research in VAWT has not been sufficiently investigated. The structure of VAWT is different from that of HAWT, vortex shedding caused by flow separation can also lead to more complex flow field and load fluctuations, reducing blade structural safety. Therefore, the aerodynamic characteristics under the synergic motion of pitch and flap need to be further studied.

In this paper, a VAWT with the synergic motion of pitch and flap will be proposed. A series of two-dimensional CFD simulations were conducted to evaluate the effects of the oscillation amplitude of pitch angle, flap deflection angle, and the position of the flap on the aerodynamic performance at different TSRs. The analysis process of the CFD methodology and post processing in this paper is shown in Fig. 1.

Methodology

Geometric model

The present work utilizes the airfoil NACA0021 model as a base case, which has been investigated in a lot of previous studies [30–32]. The struts of the wind turbine were neglected to simplify the numerical model [32]. Assuming that the the induced velocity is zero in this study [33]. The original VAWT adopts the following parameters: Airfoil type = NACA 0021, Blade number = 3, Diameter of wind turbine $D = 1.030$ m, Chord length $c = 0.0858$ m, Solidity $\sigma = 0.25$, and Swept area $A = 1.03$ m^2.

Schematic of the synergic motion of pitch and flap

In this study, an efficient combination control strategy is put forward to adjust the AOA with the synergic motion of pitch and flap. The airfoil with flap is illustrated in Fig. 2 (a), c is the chord length, x_p is the

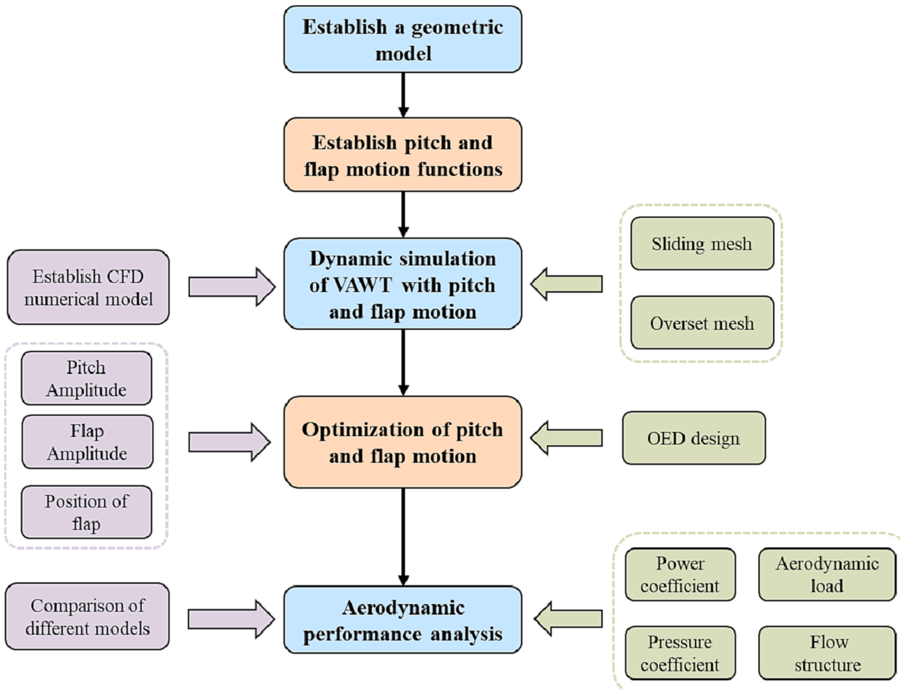

Fig. 1. The analysis process of CFD methodology and post processing for the wind turbine model.

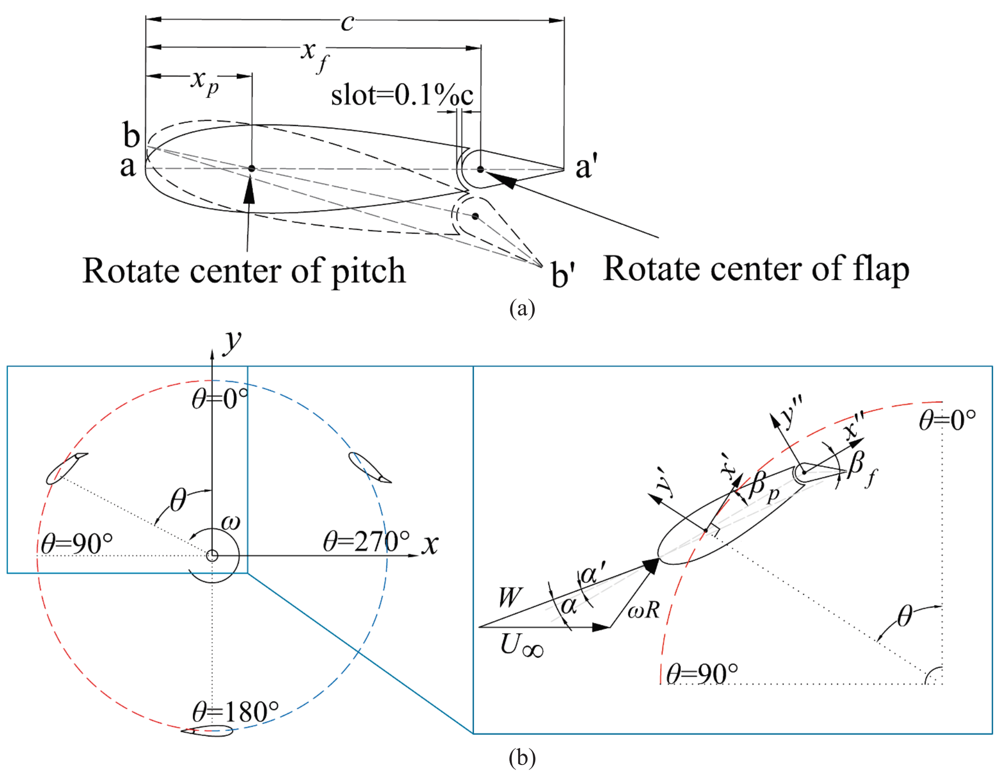

Fig. 2. The schematic of airfoil and VAWT with flap during the revolution.

distance from the leading-edge to the rotate center of the pitch which is equal to 0.25*c* in this study, x_f is the distance from the leading-edge to the rotational center of the flap, and the slot of the airfoil is 0.1 %*c* to reduce the influence of slot on airfoil aerodynamic performance.

The VAWT with flaps is shown in Fig. 2 (b). During the rotation of VAWT, the AOA is adjusted with the synergic motion of pitch and flap. The chord line of the blade is defined as the connecting line between the leading-edge point and trailing edge point. For blade without variation of pitch angle and flap angle, the original pitch angle β_p is the angle between the original blade chord line aa' and the circumferential tangent of VAWT rotation. With the oscillation of pitch and flap, the chord line of the blade changed from aa' to bb'. The angle between the new chord line bb' of the blade and the circumferential tangent of VAWT rotation can be called equivalent AOA $\alpha'(\theta)$. To control the motion of pitch and flap, three Lagrangian coordinates of the blades and three Lagrangian coordinates of flaps were established, respectively, based on the global coordinate as is shown in Fig. 3(b). The coordinates of flaps were under the management of the coordinates of blades. The pitch angle β_p and flap deflection β_f and are positive when they rotate counterclockwise. Therefore, the equivalent AOA of the blade with the synergic motion of pitch and flap can be rewritten:

$$\alpha'(\theta) = \arctan\left(\frac{sin\theta}{\lambda + cos\theta}\right) - \left(\beta_p(\theta) - \arctan\left(\frac{sin\beta_f(\theta)}{\frac{x_f}{c} + (1-\frac{x_f}{c})cos\beta_f(\theta)}\right)\right) \quad (1)$$

The specific pitch motion function is as follows:

$$\beta_p(\theta) = \begin{cases} \beta_{p1}\sin(3\theta) 0 < \theta \le \frac{\pi}{3}, and \frac{5\pi}{3} < \theta \le 2\pi \\ -\beta_{p2}\sin\left(\frac{3}{2}(\theta - \frac{1}{3}\pi)\right) \ \frac{\pi}{3} < \theta \le \frac{5\pi}{3} \end{cases} \quad (2)$$

where β_{p1} and β_{p2} are the amplitude of pitch angle.

Similarly, the motion function of the flap is:

$$\beta_f(\theta) = \begin{cases} \beta_{f1}\sin(3\theta) 0 < \theta \le \frac{\pi}{3}, and \frac{5\pi}{3} < \theta \le 2\pi \\ -\beta_{f2}\sin\left(\frac{3}{2}(\theta - \frac{1}{3}\pi)\right) \ \frac{\pi}{3} < \theta \le \frac{5\pi}{3} \end{cases} \quad (3)$$

where β_{f1} and β_{f2} are the amplitude of flap angle.

To further understand and optimize the aerodynamic performance of VAWT under the synergic motion of pitch and flap, four different models are built to evaluate the effect of the synergic motion of pitch and flap. The model without flap and motion of pitch of flap is called the base model. The model with pitch-only motion, flap-only motion, and pitch-flap synergic motion can be called the pitch-only (P-O) model, flap-only (F-O) model, and pitch-flap (P-F) model, respectively. The Specific optimization design process is introduced in the next section.

The orthogonal experiment design (OED) method

The study of the parameters related to pitch and flap is beneficial to improving the performance and load reduction ability of wind turbines. However, due to the large number of parameters affecting the performance of VAWT, the overall calculation workload is heavy, and it is not easy to compare the influence of different parameters on results. The orthogonal experimental design is a method of multi-factor test. The orthogonal experimental design requires each influencing factor and factor combination in the design to have equal opportunities to appear, and the distribution of each factor combination is balanced. Therefore, some representative points need to be selected from the comprehensive test to carry out the test.

Range analysis is commonly a used analysis method in OED. The OED requires the selection of appropriate test results to evaluate the merits of the results, called the test index. By comparing the average value of each index of this factor, the maximum value and the minimum value are found and the range of factors can be obtained by subtracting the two values, which is denoted by R. The greater R has a greater impact on the corresponding factor. Through the above process, the optimal factor and level combination for a certain test index can be determined.

In this paper, the oscillation amplitude of pitch angle, flap deflection angle, and the position of the flap that affect the aerodynamic performance of the VAWT were chosen as three factors of OED. Three levels were selected for each factor as shown in Table 1. For the original blade, the near-wall blade boundary layer separation is well developed near 4/5 chord length. Thus, the investigation of the slot location (Factor A) is performed for three slot positions of 0.75c, 0.85c, and 0.95c to control separation properly. The reasonable range of variable pitch was 2° to 20° for different TSRs [12,23,34,35]. Therefore, in this research, the levels of maximum pitch amplitude (Factor B) were 4°, 6°, and 8° considering the TSRs in this study were moderate. The flap amplitude is

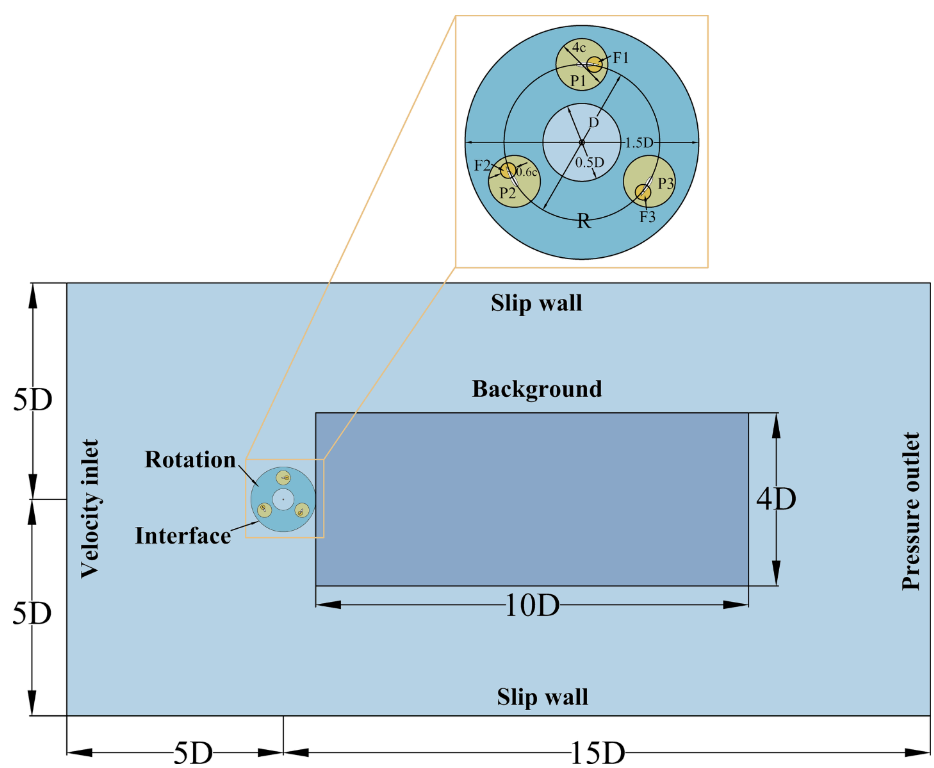

Fig. 3. Schematic layout of the computational domain.

Table 1
The factor used in the OED analysis.

Location of slot (Factor A)	Maximum pitch amplitude (Factor B)	Maximum flap amplitude (Factor C)
0.75c	4°	10°
0.85c	6°	15°
0.95c	8°	20°

another important parameter. Xiao [36] investigated an oscillating flap with an oscillating amplitude of 15° to reduce the blade wake vortex interaction. In this paper, the maximum flap amplitudes (Factor C) of 10°, 15°, and 20° were chosen to be investigated.

The purpose of the synergic motion of pitch and flap is to optimize the power output and reduce the load on VAWT. Therefore, the ratio of power coefficient C_P and thrust coefficient C_{thrust} was used as a comprehensive index ξ to evaluate the quality of optimized results:

$$\xi = \frac{C_P}{C_{thrust}} \tag{4}$$

Computational model and its validation

Computational domain and boundary conditions

The computation cost of 3D and 2.5D CFD simulations is much higher than 2D CFD simulations in the optimization problem presented in this study. Therefore, a 2D topology structure of the computational domain was established as shown in Fig. 3 to conduct the simulation, which consists of eight regions, namely, the rotational region of pitch P1 to P3, rotational region of flap F1 to F3, rotational region of VAWT, and background region. The boundary of the rotational region of VAWT which was connected to the background region was set as an interface boundary condition to simulate the rotational motion of the VAWT through sliding mesh. The mesh size on both sides of the interface was kept constant to ensure data interaction between meshes. Regions P1 to P3 and F1 to F3 were circular rotatable subdomains around the blades. The individual motions of pitch and flap were simulated by rotating overset mesh regions. Besides, regions around the flap and behind the VAWT were refined. For the boundary conditions, the upstream side of the flow field was set as an inlet boundary condition, the uniform freestream velocity $U_\infty = 9$ m/s. The downstream side of the flow field was set as an outlet condition, the relative pressure of the outlet is 0 Pa. In addition, the density of air $\rho = 1.225$ kg/m^3 and the turbulence intensity $I = 5\%$ in the inlet [32]. The wall condition on the surfaces of blades was no-slip wall condition. As the tip speed ratio $\lambda = (R\varpi)/U_\infty$ is defined as a dimensionless parameter, only the uniform freestream inlet was considered.

Numerical settings

The selection of the turbulence model has a considerable effect on the accuracy and the computational efficiency to simulate the VAWT modeling. In this study, the finite volume-based computational fluid dynamics software STAR-CCM + is used to numerically simulate unsteady incompressible two-dimensional flows. The SST k-ω turbulence model was applied to solve the Navier-Stokes equations [37]. The SST k-ω turbulence model can correctly duplicate VAWT experimental results with two-dimensional and three-dimensional models [32,38,39]. The SIMPLE (Semi-Implicit Method for Pressure-Linked Equations) algorithm was applied for coupling the pressure–velocity equation and the RANS model.

Validation

To evaluate the accuracy of the CFD results, this study uses wind tunnel experimental dates of the power coefficient C_P obtained by Castelli et al. [32,40], which has been widely used in many VAWT studies [12,35,41]. The current results compared with experiments and numerical data [12,40] is shown in Fig. 4. The power coefficient C_P is

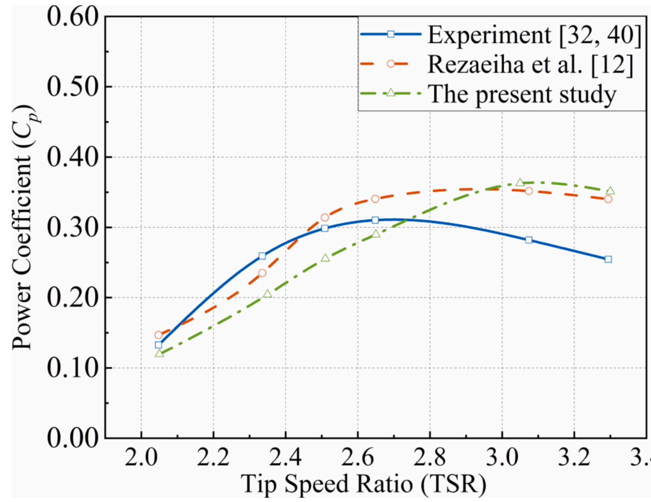

Fig. 4. Comparison of the current model against experimental and numerical data [12,32,40].

slightly overestimated for moderate to high TSRs. This may due to that the 2D CFD simulation does not take into account the effect of tip losses [42]. In addition, the value of the drag of the blades cannot be ignored for high TSRs [43]. However, the power coefficient C_P of the current results is slightly lower than the experimental data for low to moderate TSRs. It suggests that the model tends to underestimate the C_P at these operating conditions due to the geometric simplification from 3D to 2D neglecting the effect of tip losses. Another possible reason may lie on the use of SST k-ω turbulence model which would inevitably bring about numerical error for the solution of the Naiver-Stokes equation. Ismail et al. [44] also reported this tendency of underestimating airfoil performance in their studies.

Result and discussion

The results of the turbine performance under the proposed motion strategies are provided in this section. Firstly, the significance of the influence of three factors on power performance is discussed in section 3.1 through OED results. Then, in section 3.2, by adopting optimized motion strategies, the improvements in the aerodynamic features of VAWT are analyzed.

Results of OED

The optimized motion of pitch and flap can not only help improve the self-starting capability at low TSRs but also maximize the power generation at moderate TSRs. Therefore, the simulation experiments were carried out at TSR = 2.05 and TSR = 2.65 as representative points which are close to the experimental values. Further, the point of TSR = 2.05 corresponds to the starting point and the one of TSR = 2.65 to the maximum value point of the experiment in [40]. Higher discrepencies were observed at other TSR points between the experiment and numerical study, and they were not selected for further investigation.

The average values of different levels for the different factors are shown in Fig. 5 (a). Both at low TSR and high TSR, the optimal flap position is 0.95c. Therefore, in subsequent studies, the flaps were fixed at 0.95c. However, there is a significant difference in the effect of pitch amplitude on index ξ. The range values R can be obtained as is shown in Fig. 5 (b). At low TSR, with the increase of pitch amplitude from 4° to 8°, the mean values of different levels change from 0.285 to 0.359, which increase 25.9%. But at high TSR, the maximum mean values of pitch amplitude appears at 6°, which only increase 2.8% compared with pitch amplitude = 4°, and there is no significant difference between the pitch amplitude of 6° and 8°. Therefore, it is necessary to adopt different

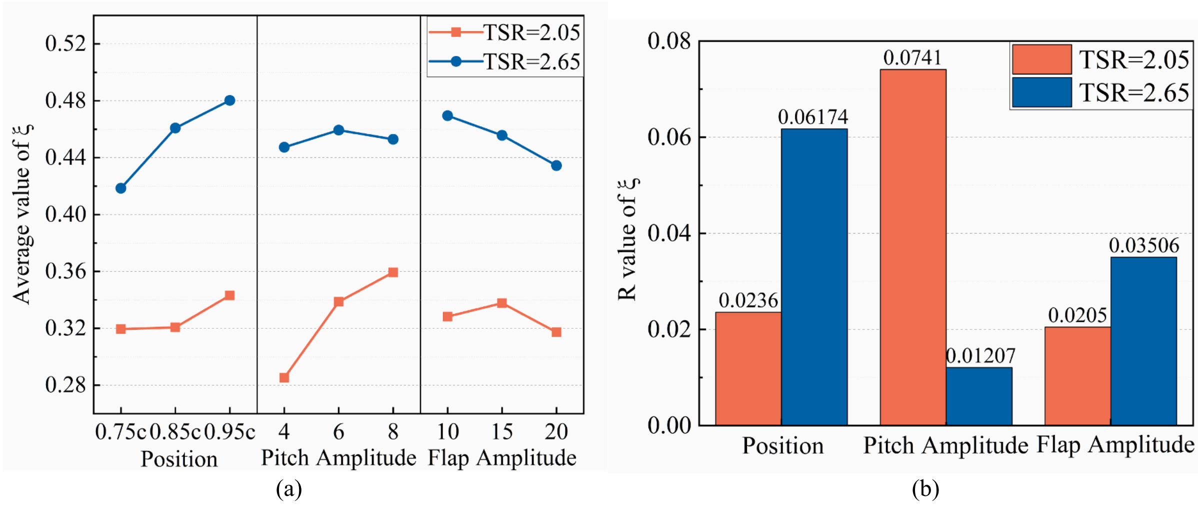

Fig. 5. The average values and range of different levels for the different factors: (a) Average values; (b) Range R.

control strategies to improve the overall efficiency of the VAWT under different TSRs. Under the low TSR, pitch control should be the primary control strategy and under the high TSR, flap control is more efficient.

Analysis of aerodynamic performance

In this section, the numerical results of VAWT with optimized P-F models for TSRs equal to 2.05 and 2.65 are compared with the P-O model, F-O model, and base model. Considering the incoming flow was disturbed in downstream half cycles of rotation, the analysis mainly focused on the upstream half cycles of rotation to help better understand the effect of the synergic motion of pitch and flap on the aerodynamic performance of VAWT.

Instantaneous force comparison

Fig. 6 (a) shows the torque coefficient versus azimuthal angle of different models at TSR = 2.05. As it was plotted, the enhancement mainly attributes to advanced performance in the first-half cycle. In most regions, the torque coefficients of the P-F and P-O model are higher than the F-O model and base model, especially in the azimuth range from 60° to 120°, where a dramatic decrease appeared in the curve of the base model due to dynamic stall. More obvious patterns can be observed at TSR = 2.65 in Fig. 6(b). In more regions, from 60° to 180°, the torque coefficient of the P-F model is higher than the other three models obviously. In addition, the torque coefficients of the F-O, P-O, and P-F model are slightly higher than the base model in the azimuth range from 0° to 60° both at TSR = 2.05 and 2.65, because the motion of

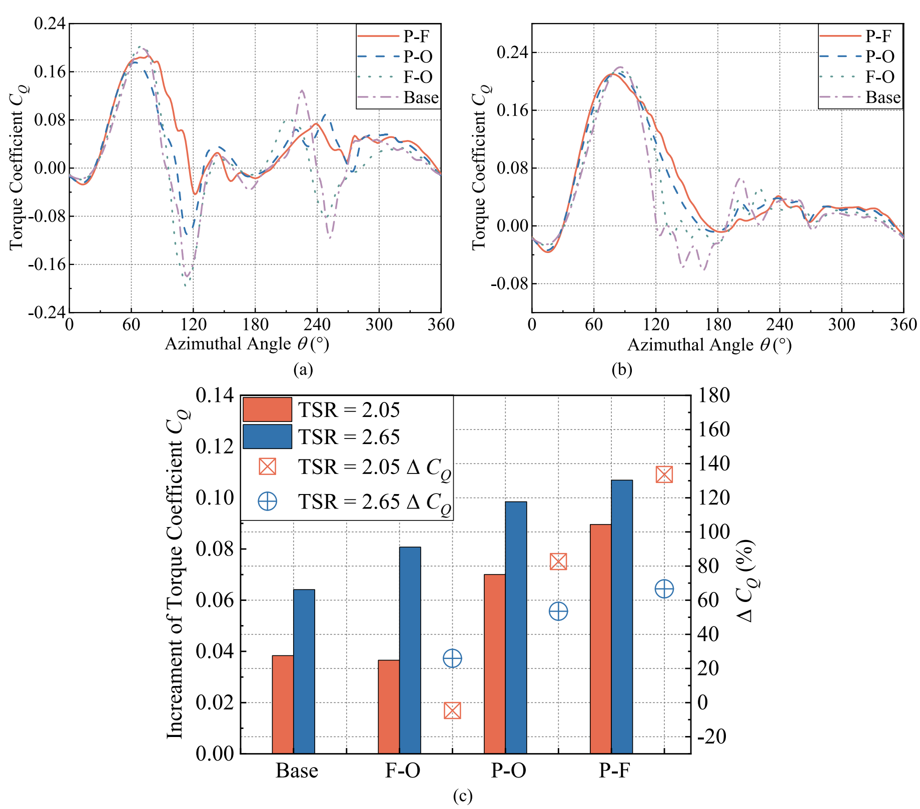

Fig. 6. The torque coefficient C_Q of one blade at (a) TSR = 2.05; (b) TSR = 2.65; (c) Increment of torque coefficient of one blade.

pitch and flap increases the AOA faster in this region. As the assumption of design in Section 2.2, the current scheme overcomes the drawbacks of the early stall and mitigates the torque loss during this period.

However, on the other hand, the effect of adopting P-O and F-O model is different for low and moderate TSRs. In both low and moderate TSRs, using the P-O model scheme also enhances the overall performance. While for the F-O model, it does not always have positive effects. At low TSR, a subtle reduction of power performance can be observed by using the F-O model compared with the base model (Fig. 6(a)), indicating that the severe stall cannot be effectively alleviated at low TSR through the F-O model. Therefore, using pitch motion to adjust the AOA of the blade is a necessary strategy to delay stall at low TSR.

Fig. 6(c) shows the increments in torque coefficient for different TSRs with different strategies. Steady improvements of C_Q can be found by using F-O, P-O, and P-F motion, where the ΔC_Q is more than 60% by using P-F motion at high TSR and impressively reaches nearly 140% at low TSR.

Fig. 7 shows the variations of the thrust coefficient C_{thrust}. Although the lowest thrust coefficient has no significant change both at TSR = 2.05 and 2.65, the maximum thrust coefficient of the optimized P-F model is lower than base model and F-O model obviously, especially at TSR = 2.65, which is helpful to reduce the load fluctuation on VAWTs during the operation.

Flow structure

Flow visualization can help understand the effect of the blade pitch and flap control on blade. The comparison of vorticity distributions at different azimuthal angles of the blade of base model and pitch model at TSR = 2.05 is illustrated in Fig. 8 (a). At the azimuthal angle $\theta = 30^\circ$ and $\theta = 60^\circ$, it can be observed that the flows are attached to the blade surface for four models. When the blade rotates to the position $\theta = 90^\circ$, the AOA of blades began to exceed the stall AOA, and different degrees of separation vortices began to appear on the blade surface of the four models. As the VAWT continued to rotate, the energy of the trailing edge reverse induced vortices gradually increased, resulting in two continuously expanding vortices at the leading edge and trailing edge of the blade. The shedding vortices generated at the leading edge of the blade gradually fall off and dissipate in the process of developing towards the middle of the blade. These separation vortices, as well as the dynamic stalling, can partly explain the torque loss of the wind turbine. The F-O motion even shows a larger vortex when θ is around 120°, explaining the corresponding drop of C_Q and C_T in Fig. 6 (a). However, the P-O model and P-F model show superiority in suppressing flow separation, and the strength of shedding vortices is smaller compared with the other models. In addition, the strongest vortex shedding of the P-F model happens around $\theta = 150^\circ$, but other three models happens around $\theta = 120^\circ$, indicating the dynamic stall is delayed.

Fig. 8 (b) illustrates the ambient vortex of blade for TSR = 2.65. The complex and chaotic vortex environment gradually becomes clear and regular by adopting F-O model, P-O model, and P-F model step-by-step. The flow separation has already been suppressed by adopting F-O model at the azimuthal angle $\theta = 120^\circ$, which is different from the condition at TSR = 2.05. The detached point moves back to the trailing edge as the motion scheme evolves.

Conclusion

The aerodynamic performance of VAWT based on synergic control of pitch and flap was numerically investigated by using the SST k-ω model and OED methods. The effects of the pitch and flap on the aerodynamic performance of VAWT were evaluated. The coefficients of forces, instantaneous vorticity contours, and static pressure distribution were investigated. Computational analysis shows that the optimized synergic motion of pitch and flap can improve the aerodynamic performance of VAWT compared to the conventional VAWT, some key findings and conclusions are listed as follows.

(1) The best aerodynamic performance of VAWT was achieved at flap position = 0.95c, pitch amplitude = 8°, and flap amplitude = 15° at TSR = 2.05, and flap position = 0.95c, pitch amplitude = 6°, and flap amplitude = 10° at TSR = 2.65, respectively.
(2) The improved sinusoidal pitch and flap motion significantly improves the characteristics of power efficiency of the VAWT at both low TSR and moderate TSR. Compared to the base model, the enhancement in torque coefficient is more than 130% and 60% for low TSR and moderate TSR, respectively.
(3) For different TSRs, it is necessary to adopt different control strategies to improve the overall efficiency of the VAWT. At low TSR, the power efficiency of the VAWT cannot be effectively improved by F-O motion. However, power efficiency improves more than 30% with F-O motion at moderate TSR. Therefore, under the low TSR, pitch control should be the primary control strategy and under the high TSR, flap control is more efficient.
(4) The improved sinusoidal pitch and flap motion can effectively inhibit the flow separation under different TSRs, and significantly improve the pressure distribution on the blade surface.

CRediT authorship contribution statement

Zhaolong Han: Writing – original draft, Methodology, Data

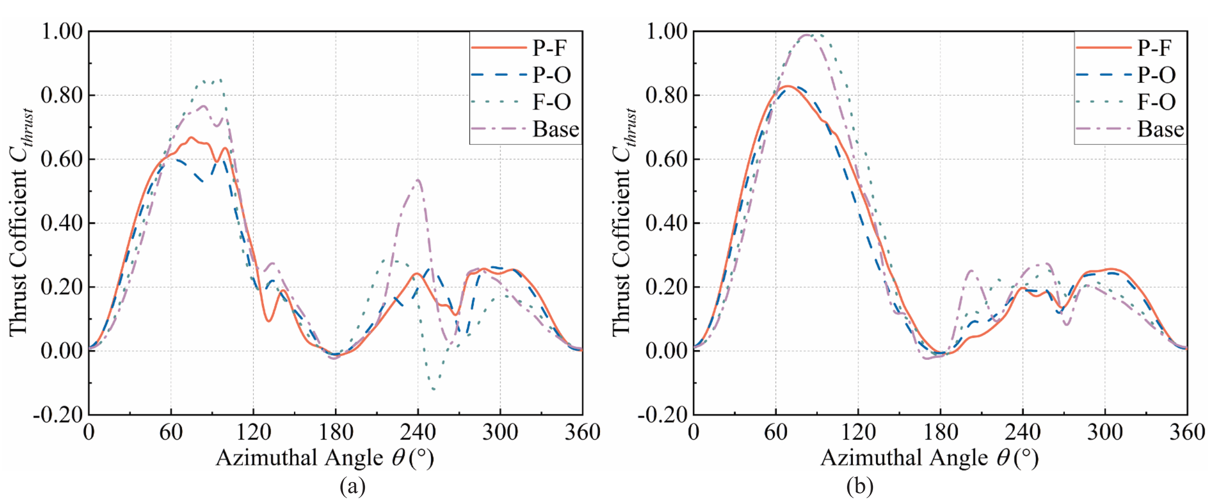

Fig. 7. The variations of the thrust coefficient C_{thrust} at (a) TSR = 2.05; (b) TSR = 2.65.

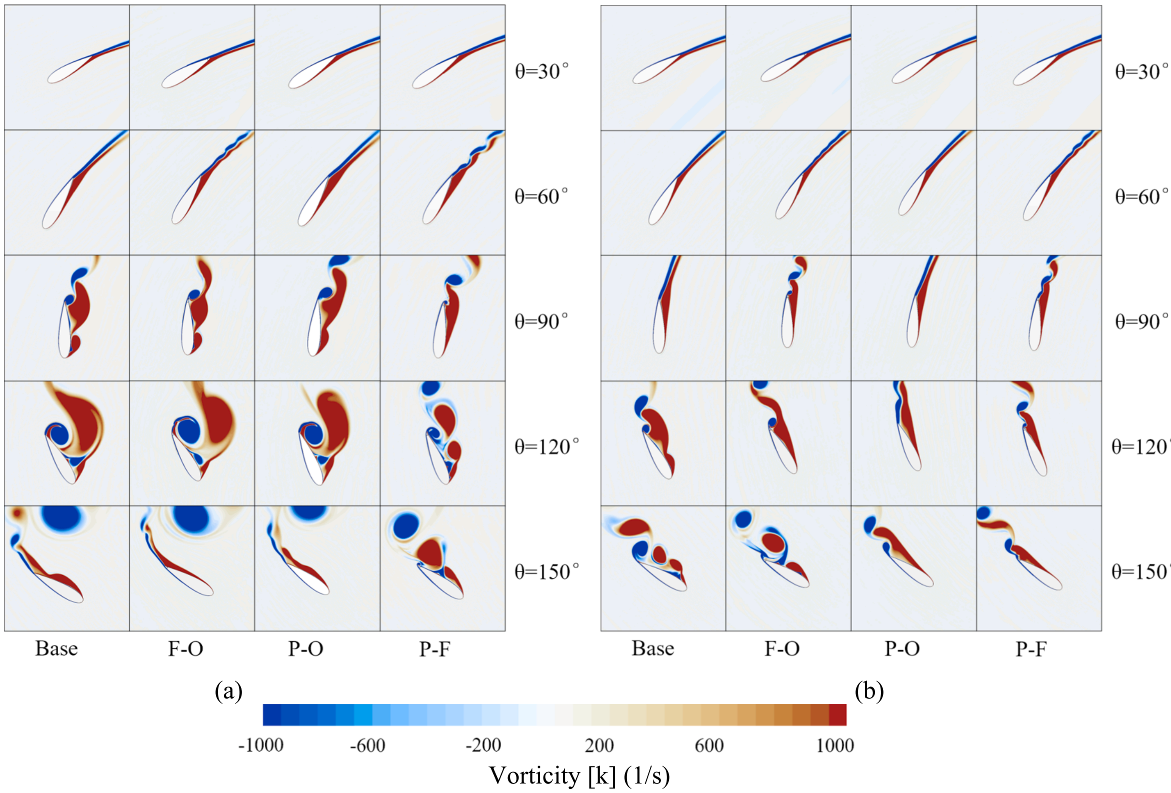

Fig. 8. The comparison of vorticity magnitude at different azimuthal angles of different models at (a) TSR = 2.05; (b) TSR = 2.65.

curation, Writing – review & editing. **Hao Chen:** Writing – original draft, Methodology, Data curation, Writing – review & editing. **Yaoran Chen:** Writing – original draft, Methodology, Writing – review & editing. **Jie Su:** Supervision, Writing – review & editing. **Dai Zhou:** Writing – original draft, Methodology, Writing – review & editing, Data curation, Writing – review & editing, Supervision. **Hongbo Zhu:** Methodology, Supervision. **Tangbin Xia:** Software, Writing – review & editing, Supervision. **Jiahuang Tu:** Writing – review & editing, Supervision.

Declaration of Competing Interest

The authors declare that they have no known competing financial interests or personal relationships that could have appeared to influence the work reported in this paper.

Data availability

Data will be made available on request.

Acknowledgments

The financial supports from National Natural Science Foundation of China (No. 52122110) and Innovation Program of Shanghai Municipal Education Commission (No.2019-01-07-00-02-E00066), as well as National Natural Science Foundation of China (Nos. 42076210, 52088102, 52101322), the Oceanic Interdisciplinary Program of Shanghai Jiao Tong University (SL2020PT201, SL2021MS008, SL2021PT302) and Hunan Provincial Natural Science Foundation of China (2021JJ50027) are gratefully acknowledged.

Appendix A. Supplementary data

Supplementary data to this article can be found online at https://doi.org/10.1016/j.seta.2023.103250.

References

[1] Mittal P, Mitra K. Determining layout of a wind farm with optimal number of turbines: A decomposition based approach. J Clean Prod 2018;202:342–59.
[2] Breton S-P, Moe G. Status, plans and technologies for offshore wind turbines in Europe and North America. Renew Energy 2009;34(3):646–54.
[3] The J, Yu H. A critical review on the simulations of wind turbine aerodynamics focusing on hybrid RANS-LES methods. Energy 2017;138:257–89.
[4] Díaz H, Guedes Soares C. Review of the current status, technology and future trends of offshore wind farms. Ocean Eng 2020;209:107381.
[5] Hand B, Kelly G, Cashman A. Aerodynamic design and performance parameters of a lift-type vertical axis wind turbine: A comprehensive review. Renew Sustain Energy Rev 2021;139:110699.
[6] Hand B, Cashman A. A review on the historical development of the lift-type vertical axis wind turbine: From onshore to offshore floating application. Sustainable Energy Technol Assess 2020;38:100646.
[7] Ottermo F, Bernhoff H. An upper size of vertical axis wind turbines. Wind Energy 2014;17(10):1623–9.
[8] Peng YX, Xu YL, Zhan S, Shum KM. High-solidity straight-bladed vertical axis wind turbine: Aerodynamic force measurements. J Wind Eng Ind Aerodyn 2019;184:34–48.
[9] Peng Y-X, Xu Y-L, Zhu S, Li C. High-solidity straight-bladed vertical axis wind turbine: Numerical simulation and validation. J Wind Eng Ind Aerodyn 2019;193:103960.
[10] Su J, Chen Y, Han Z, Zhou D, Bao Y, Zhao Y. Investigation of V-shaped blade for the performance improvement of vertical axis wind turbines. Appl Energy 2020;260:114326.
[11] Ostos I, Ruiz I, Gajic M, Gomez W, Bonilla A, Collazos C. A modified novel blade configuration proposal for a more efficient VAWT using CFD tools. Energ Conver Manage 2019;180:733–46.
[12] Rezaeiha A, Kalkman I, Blocken B. Effect of pitch angle on power performance and aerodynamics of a vertical axis wind turbine. Appl Energy 2017;197:132–50.
[13] Wang Y, Li G, Shen S, Huang D, Zheng Z. Investigation on aerodynamic performance of horizontal axis wind turbine by setting micro-cylinder in front of the blade leading edge. Energy 2018;143:1107–24.
[14] Luo D, Huang D, Sun X. Passive flow control of a stalled airfoil using a microcylinder. J Wind Eng Ind Aerodyn 2017;170:256–73.
[15] Belamadi R, Djemili A, Ilinca A, Mdouki R. Aerodynamic performance analysis of slotted airfoils for application to wind turbine blades. J Wind Eng Ind Aerodyn 2016;151:79–99.
[16] Beyhaghi S, Amano RS. A parametric study on leading-edge slots used on wind turbine airfoils at various angles of attack. J Wind Eng Ind Aerodyn 2018;175:43–52.
[17] Wang H, Zhang B, Qiu Q, Xu X. Flow control on the NREL S809 wind turbine airfoil using vortex generators. Energy 2017;118:1210–21.

[18] Meng H, Ma Z, Dou B, Zeng P, Lei L. Investigation on the performance of a novel forward-folding rotor used in a downwind horizontal-axis turbine. Energy 2020;190:116384.
[19] Sagharichi A, Ghaghelestani TN, Toudarbari S. Impact of harmonic pitch functions on performance of Darrieus wind turbine. J Clean Prod 2019;241:118310.
[20] Chen B, Su S, Viola IM, Greated CA. Numerical investigation of vertical-axis tidal turbines with sinusoidal pitching blades. Ocean Eng 2018;155:75–87.
[21] Jain P, Abhishek A. Performance prediction and fundamental understanding of small scale vertical axis wind turbine with variable amplitude blade pitching. Renew Energy 2016;97:97–113.
[22] Abdalrahman G, Melek W, Lien FS. Pitch angle control for a small-scale Darrieus vertical axis wind turbine with straight blades (H-Type VAWT). Renew Energy 2017;114:1353–62.
[23] Li C, Xiao Y, Xu YL, Peng YX, Hu G, Zhu S. Optimization of blade pitch in H-rotor vertical axis wind turbines through computational fluid dynamics simulations. Appl Energy 2018;212:1107–25.
[24] Liggett N, Smith MJ. The physics of modeling unsteady flaps with gaps. J Fluids Struct 2013;38:255–72.
[25] Petz R, Nitsche W. Active Separation Control on the Flap of a Two-Dimensional Generic High-Lift Configuration. J Aircr 2007;44(3):865–74.
[26] Zhu H, Hao W, Li C, Ding Q. Effect of flow-deflecting-gap blade on aerodynamic characteristic of vertical axis wind turbines. Renew Energy 2020;158:370–87.
[27] Hao W, Li C. Performance improvement of adaptive flap on flow separation control and its effect on VAWT. Energy 2020;213:118809.
[28] Liu Q, Miao W, Li C, Hao W, Zhu H, Deng Y. Effects of trailing-edge movable flap on aerodynamic performance and noise characteristics of VAWT. Energy 2019;189:116271.
[29] Chen ZJ, Stol KA, Mace BR. Wind turbine blade optimisation with individual pitch and trailing edge flap control. Renew Energy 2017;103:750–65.
[30] Li Q, Maeda T, Kamada Y, Murata J, Furukawa K, Yamamoto M. Effect of number of blades on aerodynamic forces on a straight-bladed Vertical Axis Wind Turbine. Energy 2015;90:784–95.
[31] He J, Jin X, Xie S, Cao Le, Wang Y, Lin Y, et al. CFD modeling of varying complexity for aerodynamic analysis of H-vertical axis wind turbines. Renew Energy 2020;145:2658–70.
[32] Castelli MR, Ardizzon G, Battisti L, Benini E, Pavesi G. Modeling strategy and numerical validation for a Darrieus vertical axis micro-wind turbine. ASME 2010 international mechanical engineering congress and exposition: Citeseer; 2010. p. 409-418.
[33] Paraschivoiu I. Wind turbine design with emphasis on Darrieus concept. 2002.
[34] Sagharichi A, Maghrebi MJ, ArabGolarcheh A. Variable pitch blades: An approach for improving performance of Darrieus wind turbine. J Renewable Sustainable Energy 2016;8(5):053305.
[35] Chen L, Yang Y, Gao Ye, Gao Z, Guo Y, Sun L. A novel real-time feedback pitch angle control system for vertical-axis wind turbines. J Wind Eng Ind Aerodyn 2019;195:104023.
[36] Xiao Q, Liu W, Incecik A. Flow control for VATT by fixed and oscillating flap. Renew Energy 2013;51:141–52.
[37] Edwards JM, Angelo Danao L, Howell RJ. Novel experimental power curve determination and computational methods for the performance analysis of vertical axis wind turbines. J Sol Energy Eng 2012;134(3):031008.
[38] Howell R, Qin N, Edwards J, Durrani N. Wind tunnel and numerical study of a small vertical axis wind turbine. Renew Energy 2010;35(2):412–22.
[39] Wang S, Ingham DB, Ma L, Pourkashanian M, Tao Z. Numerical investigations on dynamic stall of low Reynolds number flow around oscillating airfoils. Comput Fluids 2010;39(9):1529–41.
[40] Raciti Castelli M, Englaro A, Benini E. The Darrieus wind turbine: Proposal for a new performance prediction model based on CFD. Energy 2011;36(8):4919–34.
[41] Sagharichi A, Zamani M, Ghasemi A. Effect of solidity on the performance of variable-pitch vertical axis wind turbine. Energy 2018;161:753–75.
[42] Siddiqui MS, Durrani N, Akhtar I. Quantification of the effects of geometric approximations on the performance of a vertical axis wind turbine. Renew Energy 2015;74:661–70.
[43] Elkhoury M, Kiwata T, Aoun E. Experimental and numerical investigation of a three-dimensional vertical-axis wind turbine with variable-pitch. J Wind Eng Ind Aerodyn 2015;139:111–23.
[44] Ismail MF, Vijayaraghavan K. The effects of aerofoil profile modification on a vertical axis wind turbine performance. Energy 2015;80:20–31.